Nano Res (2008) 1: 46–55
DOI 10.1007/s12274-008-8002-y
Research Article

Au/$LaVO_4$ Nanocomposite: Preparation, Characterization, and Catalytic Activity for CO Oxidation

Junfeng Liu[1], Wei Chen[1], Xiangwen Liu[2], Kebin Zhou[2], and Yadong Li[1] (✉)

[1] Department of Chemistry, Tsinghua University, Beijing 100084, China
[2] College of Chemistry and Chemical Engineering, Graduate University of the Chinese Academy of Sciences, Beijing 100049, China

Received: 14 April 2008 / Revised: 8 May 2008 / Accepted: 9 May 2008

ABSTRACT

The size of the gold particles is a very important parameter to get active catalysts. This paper reports a novel colloidal deposition method to prepare Au/$LaVO_4$ nanocomposite catalyst with monodispersed Au colloids and uniform $LaVO_4$ nanoplates in nonpolar solvent. Monodispersed Au colloids with tunable size (such as 2, 5, 7, 11, 13, and 16 nm) and $LaVO_4$ nanocrystals with well-defined shapes were pre-synthesized assisted with oleic acid/amine. During the following immobilization process, the particle size and shape of Au and $LaVO_4$ were nearly preserved. As-prepared Au/$LaVO_4$ nanocomposite showed high catalytic activity for CO oxidation at room temperature. Since sizes of gold particles were well-defined before the immobilization process, size effect of gold particles was easy to be investigated and the results show that 5-nm Au/$LaVO_4$ nanocomposite has the highest activity for CO oxidation. This synthetic method can be extended further for the preparation of other composite nanomaterials.

KEYWORDS

Au/$LaVO_4$, nanocomposite, colloidal deposition, catalytic activity

Introduction

Recently, the preparation of an artificially designed structure of nanoparticles with new properties has attracted the attentions of many researchers [1, 2]. Nanocomposites with well-defined structures prepared from tailored nanoparticles provide opportunities for optimizing properties of materials and offer possibilities for observing interesting and potentially useful new properties.

Au/oxide nanocomposite has been discovered possessing surprisingly high catalytic activity at low temperature, which is dependent on the size of the gold particle, nature of the supports, and preparation methods [3–7]. However, the majority of the studies on practical applications were carried out using Au catalysts prepared via a simple deposition-precipitation method [8–10], which prevents us from getting a clear evaluation of the gold effects. Gold particles generated from this conventional process are normally polydispersed, gold-particle size and the support are interdependent, and even reproducibility of the synthesis is not always guaranteed. In order to shed light on the size and support effects in the CO oxidation reaction, it is necessary to develop a new route to obtain catalysts in which the effects on

Address correspondence to ydli@tsinghua.edu.cn

the catalytic activity could be isolated from the preparation process. Moreover, most oxide supports are structurally non-uniform; thus, the structures of supported metal materials are not well understood. In addition, increasingly gained experimental evidence continues to show that the surface structure and surface active sites, which have a direct relationship with the crystal planes of support, play an important role in determining the performance of catalysts [11–14]. Nowadays, some morphology controlled synthetic methods are established to produce high-quality and size-tunable nanoparticles which is redispersible in nonpolar solvent [15–17]. Preparation of gold composite with Au particles of controllable size and well-defined supporting nanocrystals as building blocks become more approachable.

Rare earth orthovanadates constitute an important compound family of inorganic material that has a wide application potential in catalysts [18, 19], but few investigations have been carried out on their role of supports for gold nanocatalysts. Recently, through an facile oleic acid assisted solvothermal method, we successfully synthesized uniform $LaVO_4$ nanocrystals (NCs), which share a square-plate morphology, preferentially expose (001) planes at the surface, and can be readily dispersed in nonpolar solvents [20, 21]. It would be interesting to investigate gold on uniform $LaVO_4$ NCs of controlled size, which form a more well-defined nanocatalyst and might provide special catalytic activity.

In this paper, Au/$LaVO_4$ nanocomposite was synthesized by a novel colloidal deposition method in nonpolar solvent system. Different from the colloidal deposition method in aqueous solution, our approach is based on a nonpolar solvent, which could make the uniform particles and high gold concentration available. Colloidal Au with tunable size and $LaVO_4$ nanocrystals (NCs) with well-defined morphology were prepared assisted with long chain surfactant molecules, dispersible in organic solvent. As-prepared Au/$LaVO_4$ nanocomposite which showed high catalytic activity and size effect of Au composite for CO oxidation were investigated. There may be important implications from such an investigation on the designed preparation of advanced nanostructure composites and other chemical materials.

1. Experimental

1.1 Chemicals

All the chemicals were of analytical grade and used as received without further purification. Oleylamine was purchased from ACROS ORGANICS, and all other chemicals were purchased from the Beijing Chemical Reagents Company.

1.2 Preparation of $LaVO_4$ NCs

$LaVO_4$ nanocrystals were prepared by hydrothermal method [20]. A 1-mL solution of 1 mmol $La(NO_3)_3 \cdot 6H_2O$ was added to a solution of 0.6 g NaOH, 0.06 g NH_4VO_3, 5 mL water, 10 mL oleic acid, and 10 mL ethanol under stirring. Then the mixture was transferred into a 40-mL Teflon-lined vessel, which was sealed in an autoclave and then treated for about 8 h at 140 °C. After the autoclave was cooled to room temperature naturally, the samples could be directly collected at the bottom of the vessel. The NCs were further purified by dispersed into 10 mL of cyclohexane and precipitated by addition of 10 mL of ethanol.

1.3 Preparation of Au colloids

The colloidal gold solutions were prepared using oleic acid assisted solution method. The preparation of 5- and 7-nm Au colloids followed the oil/water interface reaction procedure in normal microemulsions [22]. Different co-solvents (dimethyl formamide (DMF) or ethanol) were used to achieve 5- and 7-nm gold particles. In a typical synthesis, 30 mL aqueous solution contained 0.05 g $HAuCl_4$, 1.5 g sodium oleate, 2 mL oleic acid, and 20 mL DMF which were mixed at room temperature under vigorous agitation. A following injection of an aqueous solution of ascorbic acid (Vc) (0.05 mol/L, Au/Vc=1:2) led to graduate formation of a purple solution, indicating the formation of the gold sol. Then 20 mL cyclohexane was added immediately. The solution was continuously stirred for about 1 h and remained stable for 24 h. The gold colloids were extracted in the cyclohexane phase.

Gold colloids with larger size were synthesized assisted with oleylamine. In a typical synthesis, a solution of 10 mg tetrachloroauric acid in 1 mL oleylamine was added into 10 mL cyclohexane,

sealed in a Teflon autoclave, solvothermal treated at a temperature of 70–180 °C for 10 h. Gold nanoparticles with size of 11, 13, and 16 nm were obtained at 70, 100, and 140 °C, respectively. 2-nm gold colloids were obtained by adding 20 μL dodecanethiol to the system and treated at 100 °C for 10 h.

1.4 Preparation of Au/$LaVO_4$ composite

The cyclohexane solution of $LaVO_4$ and Au colloids was mixed with desired ratio. The mixed solution was ultrasonic treated for about half an hour to achieve the total mixture. Excess alcohol was added to the solution to precipitate the Au/$LaVO_4$. The solids were collected at the bottom of the vessel and dried at 50 °C under vacuum for 24 h. Finally, the samples were calcined in air at 250 °C for 6 h.

1.5 Materials characterization

The powder X-ray diffraction (XRD) was performed on a Bruker D8-Advance X-ray diffractometer with CuKα radiation (λ =1.5418 Å). The size and morphology of the NCs were determined by a JEOL JEM-1200EX transmission electron microscope (TEM) at 120 kV with a tungsten filament at an accelerating voltage of 120 kV and a Tecnai G2 F20 S-Twin high-resolution transmission electron microscope (HRTEM) at 200 kV. To obtain suitable samples for TEM characterization, the samples were treated as follows: colloidal solutions were first diluted with cyclohexane. Solid catalysts were finely powdered and then dispersed in ethanol solution under ultrasonic for 15 min. A drop of solution was then deposited onto a holey copper carbon grid in the native form. Energy dispersive X-ray analysis (EDXA) was used to determine the gold content of the catalysts, which was performed on a Sirion 200 scanning electron microscope equipped with an EDXA system. The BET surface area of catalysts was measured by N_2 adsorption with the single-point method.

1.6 Catalytic activity evaluation

The catalytic activities for CO oxidation were evaluated in a fixed-bed quartz tubular reactor. The catalyst particles (0.2 g) were placed in the reactor. The reactant gases (1.0% CO, 16% O_2, and balanced with nitrogen) went through the reactor at a rate of 100 mL/min. The composition of the gas exiting the reactor was monitored by gas chromatography. The operation temperature was controlled with a thermocouple and could be adjusted in the range from room temperature to 700 °C. Temperature for 50% conversion ($T_{50\%}$) as an index was chosen to evaluate the activity of the catalysts.

2. Results and discussion

Colloidal deposition method is an interesting approach by using monodispersed gold sols whose particle size is established before deposition on the oxide support to overcome the complexity related to the preparation methods so far employed [23–27]. However, pervious commonly used methods are based on aqueous solution, in which uniform particles and high gold concentration are hard to be obtained. Recently, the method of using monodispersed gold nanoparticles in aprotic solvent might provide a solution, but dispersion of hydrophobic gold nanoparticles on hydrophilic oxides was a key problem [28]. Here, via the novel nonpolar solvent-based colloidal deposition method, Au/$LaVO_4$ nanocomposite with high quality Au particles of controllable size and well-defined supporting nanocrystals as building blocks was successfully achieved. Both Au colloids and $LaVO_4$ nanocrystals had hydrophobic surfaces, so the homogeneous dispersion of gold could be easily formed by the interaction of long alkyl chains capped their surfaces.

Typical X-ray diffraction (XRD) patterns of colloidal $LaVO_4$ NCs are shown in Fig. 1(a). All the reflection peaks can be easily indexed as pure, tetragonal zircon structure [space group: $I4_1/amd$] with cell parameters: a=b=7.49 Å, c=6.59 Å, which are consistent with literature values (JCPDS Card number: 32-0504). No peaks of any other phases or impurities were detected. It is found that the (200), (220), and (400) reflections show distinct peak widths that are narrower than those of the others, indicating the larger sizes perpendicular to them for the NCs. The transmission electron microscope (TEM) and high resolution TEM (HRTEM) images of $LaVO_4$ NCs have been taken directly from the cyclohexane solution shown in Figs. 1(b), (c) . The NCs are square

plates in shape with a size of about 40 nm × 40 nm × 10 nm, preferentially exposed (001) planes [20]. The Brunauer-Emmett -Teller (BET) surface area of $LaVO_4$ NCs is 64.7 m^2/g.

Gold nanocrystals are full of promises for optical, electronic, magnetic, catalytic, and biomedical applications nowadays, by utilizing the "bottom-up" approach with the hybrid organic-inorganic building blocks derived therefrom [2, 29]. The variety of synthetic possibilities made monodispersed Au nanocrystals obtainable [15, 30, 31]. However, monodispersed gold colloids with particle size less than 10 nm in high concentration were still hard to achieve. In this paper, a novel oil/water interface reaction in normal microemulsions (water/sodium oleate/oleic acid) was developed to prepare the monodispersed gold colloids. Owing to the large solubility of the source materials in the water phase, the colloidal nanoparticles can easily be prepared on a large scale. Figures 2(a), (b) show TEM images of monodispersed Au colloids with mean particle sizes of 5 and 7 nm, respectively. High-resolution

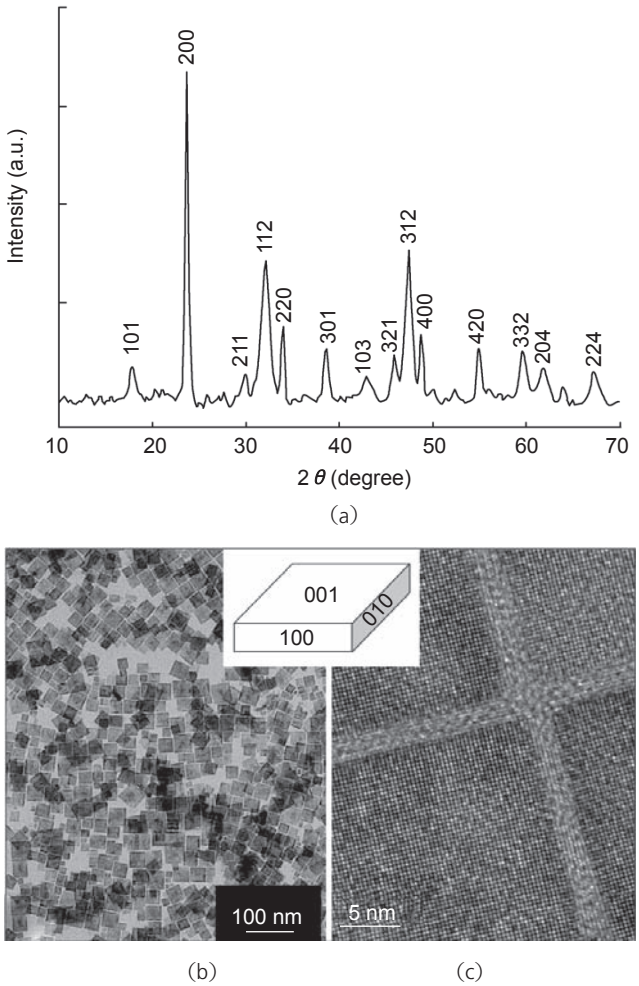

Figure 1 (a) XRD patterns of $LaVO_4$ NCs. (b), (c) TEM and HRTEM images of $LaVO_4$ nanocrystals (Inset, the schematic diagram of an individual nanoplate)

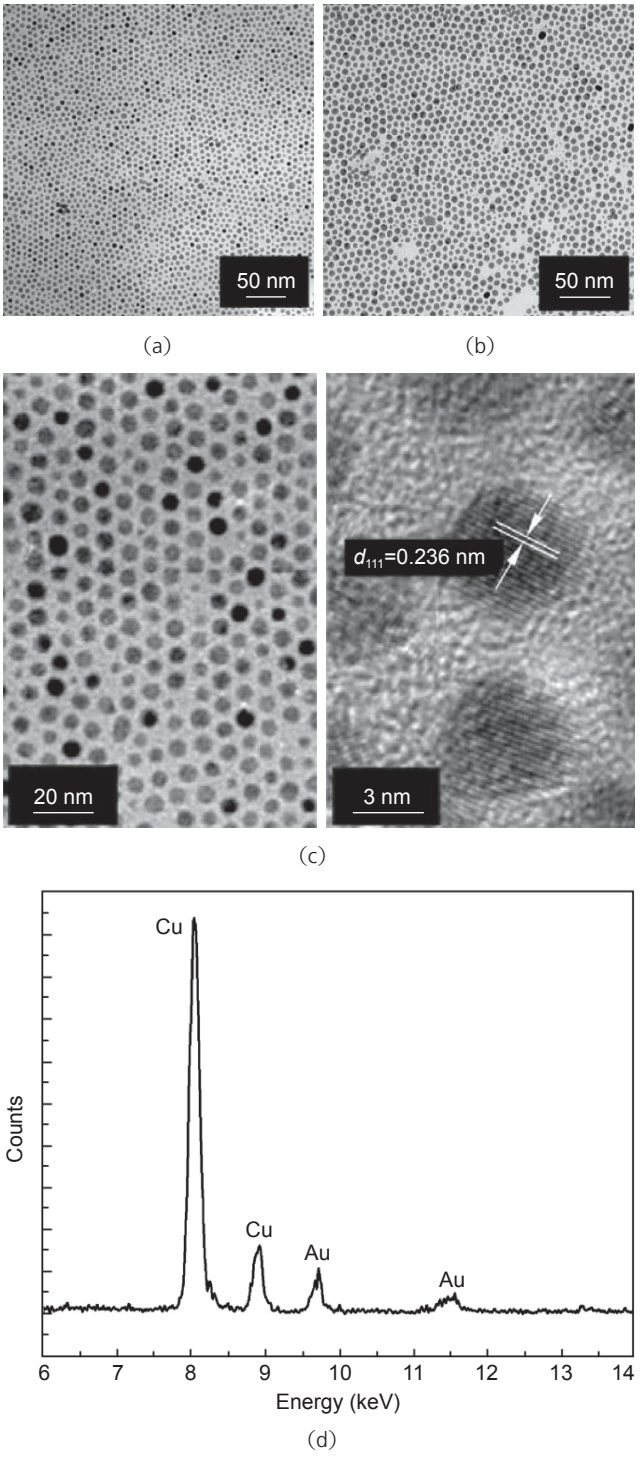

Figure 2 TEM images of Au colloids with different size: (a) 5 nm, (b) 7 nm, (c) HRTEM image of Au NCs with 5 nm, and (d) EDXA spectra of Au colloids

TEM (HRTEM) and energy dispersive X-ray analysis (EDXA) were also measured to confirm the composition and crystallization of the gold crystals (Figs. 2(c), (d)). It can be seen from the HRTEM image of Au nanoparticles that all Au nanoparticles show lattice images originating from a single crystal. The lattice spacing of 0.236 nm is in consistency with that of the bulk Au (111) plane. The brightness of the nanoparticles varies in low-magnification TEM images because the lattice planes of each particle are randomly arranged.

In the synthesis process, water, sodium oleate, oleic acid, and co-solvent form a normal microemulsion system. After adding of $HAuCl_4$ and stirring for about 5 min, the yellow color of the solution faded out, indicating the formation of coordination compounds between Au ions and oleic acid molecules at the interface of water/oil. Then following injection of ascorbic acid (Vc) led to the reduction of Au ions at interface and graduate formation of a purple solution indicating the formation of the gold sol. The in-situ generated Au nanocrytals would be covered with the long alkyl chains and thus had hydrophobic surfaces, which were incompatible with the hydrophilic surrounding of the aqueous solution. So as a result, these hydrophobic nanocrystals would be stay at the interface of water/oil and extracted into nonpolar solvents following added, such as cyclohexane. Different co-solvents could lead to different particle sizes of gold. For example, DMF led to 5 nm gold colloids, and ethanol was used to achieve 7 nm gold. Larger particle size is due to the weak reductivity of ethanol.

Gold colloids with much larger size were easily synthesized via a solvothermal reaction assisted with oleylamine. Oleylamine was present to reduce Au ion, control the growth of the nanoparticles, and give the products solubility in organic solution after their synthesis. Gold colloids with size larger than 10 nm were obtained using this solvothermal reaction. Gold nanoparticles with size of 11, 13, and 16 nm were obtained at 70, 100, and 140 °C, respectively. Lower reaction temperature below 60 °C led to incomplete reaction and larger size distribution. Figures 3(a)–(c) show TEM images of monodispersed Au colloids with mean particle sizes of 11, 13, and 16 nm, respectively. 2-nm gold colloids were obtained by adding 20 μL dodecanethiol in the system (Fig. 3(d)). The UV-vis spectra of the cyclohexane solution of as-prepared gold nanoparticles with different average sizes are shown in Fig. 4. The intensity of the absorption peak at around 530 nm originated from surface plasmon increases with an increase in the particle size, accompanied by a decrease in the peak width. Such observed features coincide with the prediction of the Mie thoery [32]. Spectrum curve (2 nm) does not show a plasmon band at all, indicating that most particles are below ca. 3 nm in size. Weak surface plasmon absorption in curve (5 nm) suggests

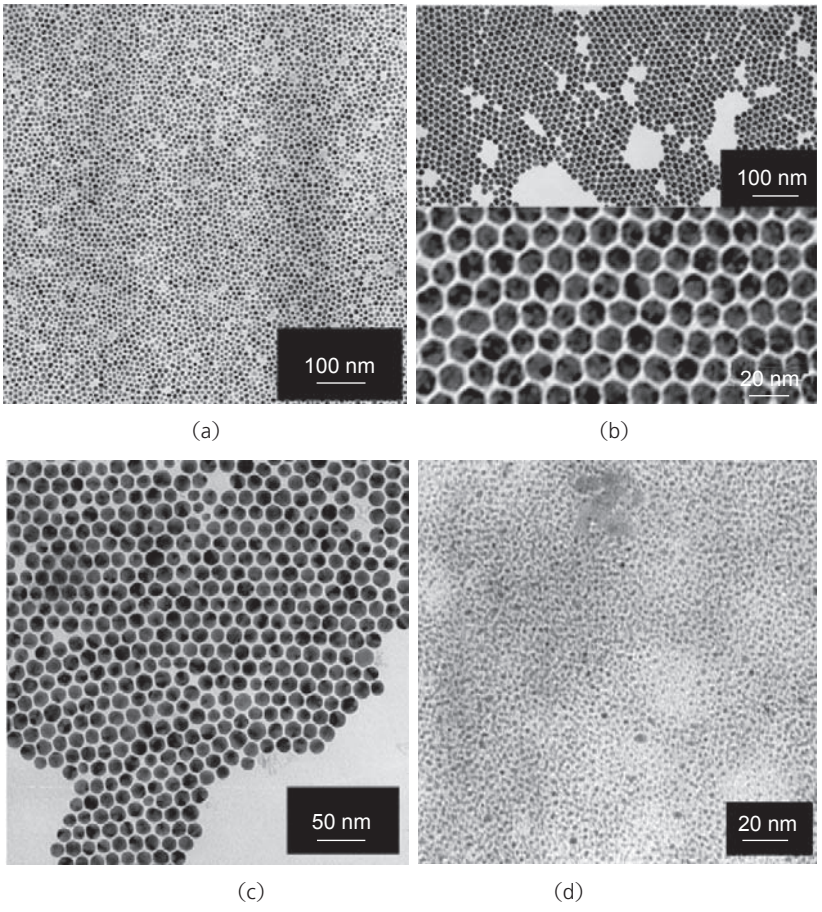

Figure 3 TEM images of Au colloids with different size: (a) 11 nm, (b) 13 nm, (c) 16 nm, and (d) 2 nm

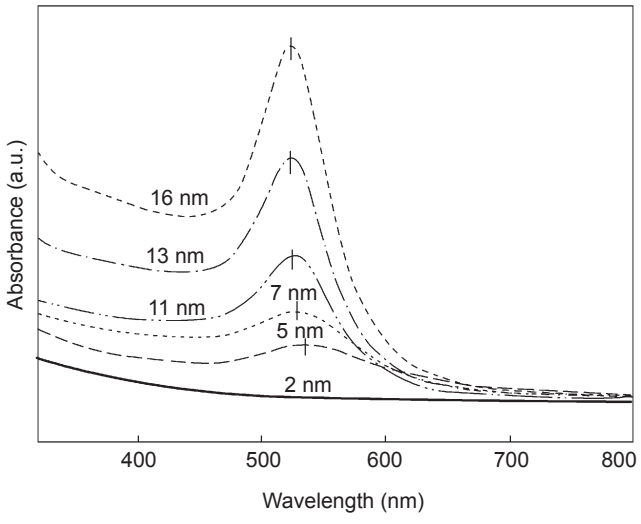

Figure 4 UV-vis spectra of the cyclohexane solution of as-prepared gold nanoparticles with different sizes (2, 5, 7, 11, 13, and 16 nm)

the formation of small particles, which is well consistent with the results from TEM observation. These nanoparticles can easily form 2-D superlattices on a flat carbon-coated copper grid probably because of van der Waals attractive forces between the Au nanoparticles.

Gold nanoparticles maintained the same size after deposition on the lanthanum vanadates NCs. Figure 5 shows TEM and HRTEM images of mixed colloids of 5-nm Au/$LaVO_4$ nanocrystals, as well as 5-nm Au/$LaVO_4$ composite after calcined at 250°C for 6 h. By mixing the cyclohexane solution of Au and $LaVO_4$ colloids with a desired ratio, the gold and $LaVO_4$ nanocrystals could link with each other through the interaction of long chain organic molecule attached on the surface (Figs. 5(a), (b)). It was noticed that there were many Au particles outside the substrates in Fig. 5(a). However, after adding excess alcohol which is a polar solvent, the solution became clear gradually along with the precipitation of Au/$LaVO_4$ nanocomposite, indicating that most of Au particles were deposited on the $LaVO_4$ nanoplates. The samples were calcined in air at 250 °C for 6 h to remove the organic species that protected the NCs in preparation. As one can see, the gold nanoparticles are characterized almost by the same particle-size distribution observed in the native solution (Figs. 5(c)–(d)). It can be seen clearly that there was no obvious growth or sintering of the Au nanoparticles on the $LaVO_4$ nanoplates during calcinations. However, adsorption on the $LaVO_4$ nanoplates does seem to change the shape of these gold nanoparticles. The particles clearly appear to be faceted after adsorption on the supporting

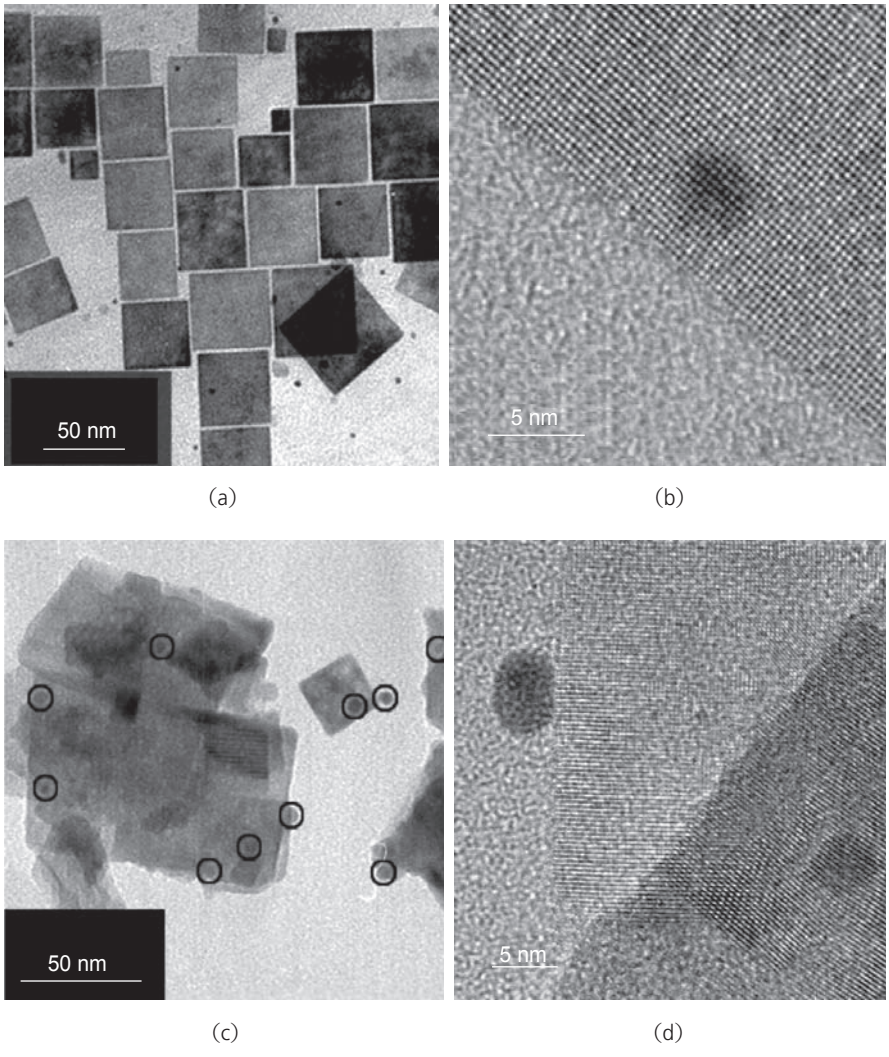

Figure 5 TEM and HRTEM images of (a), (b) 5-nm Au/$LaVO_4$ colloids before precipitation and (c), (d) 5-nm Au/$LaVO_4$ composite after calcined at 250 °C, respectively

materials, while being spherical in the native solution. The EDXA was also performed to verify the composition of sample of 2-nm Au/$LaVO_4$ composite after calcined at 250 ˚C because dodecane-thiol was used in preparation process. It is confirmed that there are only Au, La, V, and O existing in the sample and no S signal was detected.

The catalytic activity for CO oxidation was measured from low conversion to 100% conversion for the Au/$LaVO_4$ nanocomposite with different Au particle sizes. Figure 6 shows the size effect of gold on CO conversion over Au/$LaVO_4$ catalyst calcined at 250 ˚C with the same Au loading amount of 3 wt%. The activities of $LaVO_4$ supported Au nanocatalyst for CO oxidation are comparable with that of Au nanocatalyst with some oxide supports [33, 34]. As expected, the Au/$LaVO_4$ nanocomposite with different Au particle sizes and distributions have different activities. Particle size effects in CO oxidation have previously been observed for Au on oxides and it is well accepted that only gold particles with diameter lower than 5 nm are catalytically active [35]. The reaction studies indeed show a marked size effect of the catalytic activity on CO oxidation of Au/$LaVO_4$ nanocomposite, with Au particles in the range of 5 nm exhibiting the maximum reactivity. At 30 ˚C, the percentage CO conversion is 29% over 5 nm Au/$LaVO_4$ nanocomposite, and the corresponding rate of conversion of CO is 1.2 μmol/(g·s). With the varying of size from 16 nm to about 5 nm, the activity increases and the temperature of half conversion ($T_{50\%}$) decreases from 195 ˚C to 35 ˚C. These results well consist with the work of Goodman's group [35], who studied the size dependence of gold clusters on single crystalline surfaces of titania in

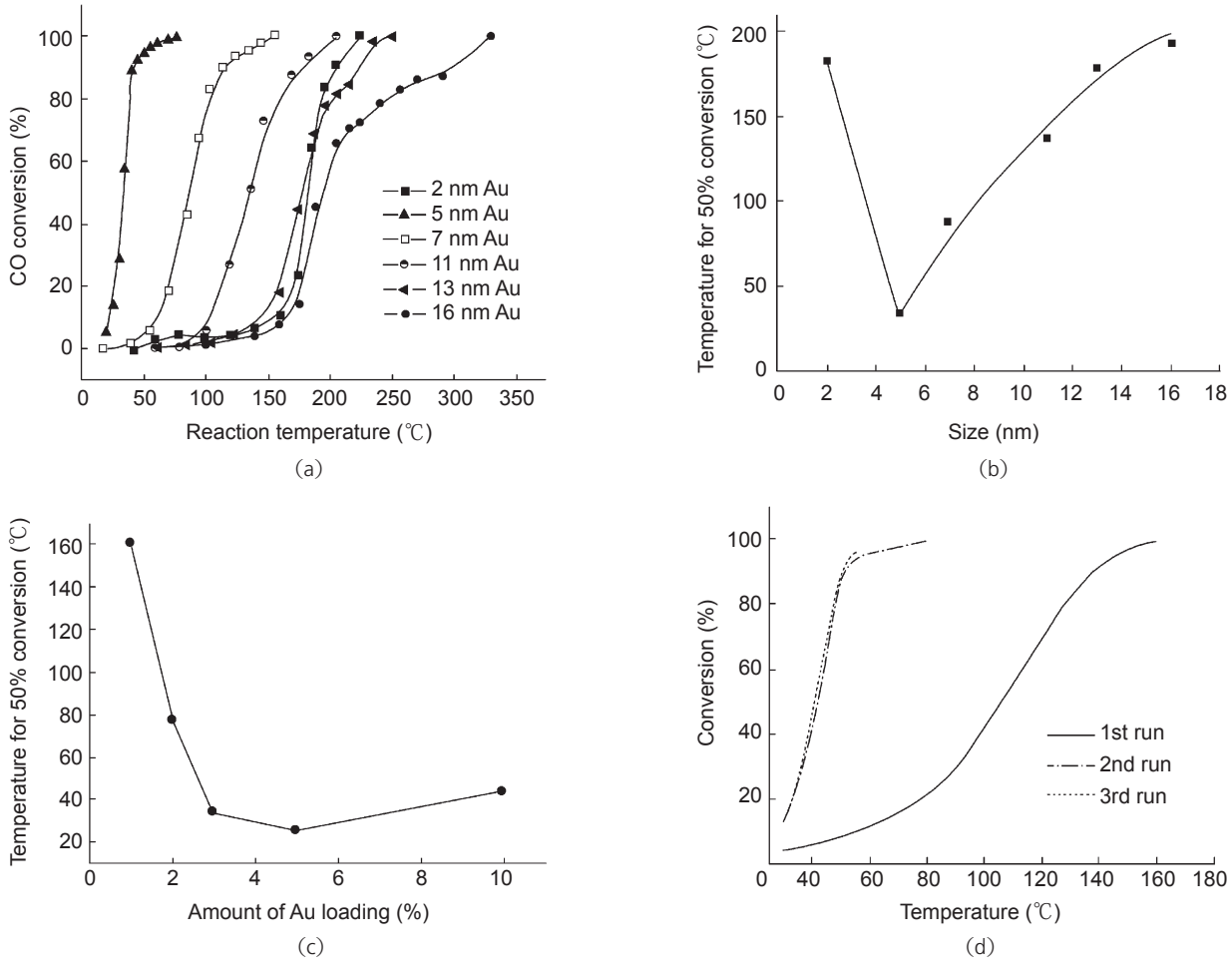

Figure 6 (a) Percentage conversion versus temperature plots for the oxidation of CO over Au/$LaVO_4$ composites with different gold particle sizes (Au loading amount: 3 wt%). (b) The influence of gold particle size on activity of CO oxidation. (c) $T_{50\%}$ versus amount of Au on 5-nm Au/$LaVO_4$ nanocomposite. (d) Activity results for Au/$LaVO_4$ (3 wt%, 5 nm) composite

ultrahigh vacuum and showed that the structure sensitivity was related to a quantum size effect with respect to the thickness of the gold islands. The activity decreases rapidly as the particle size is reduced to below 3 nm due to the occurrence of a metal-to-nonmetal transition.

For the further investigation of the catalytic activity of $Au/LaVO_4$ composite, the different gold loaded samples changing from 1 wt% to 10 wt% were used, and the results are shown in Fig. 6(c). Heating of the nanocomposite in the diluted reaction gas, containing a mixture of carbon monoxide and oxygen, interestingly revealed that 5 wt% Au loading samples had the highest catalytic activity. For the 5 wt% $Au/LaVO_4$ composite, the temperature of half conversion ($T_{50\%}$) was 25 ˚C and full conversion temperature was 45 ˚C, while the catalyst with 1 wt% Au loads amount showed 50% CO conversion at 159 ˚C and full conversion at 240 ˚C. The low CO conversion with the lowest gold loading is due to the limited availability of active component, whereas the slight decrease of high gold loading amount (10 wt%) might due to the small agglomeration of Au nanoparticles.

It has been reported that the catalysts prepared via colloids deposition method require a thermal activation, probably due to the inhibitory effect of the protecting agent that is present on the catalyst. And after samples were calcined in air at 250 ˚C for 4 h, the $Au/LaVO_4$ nanocomposite did not show any difference between the first and the following runs [25]. However, the gold nanocomposites in our results seemed to require a thermal activation, although already calcined in air at 250 ˚C for 6 h to combust the organic species. For all the samples, the results of the first run were substantially different from the results for subsequent temperature cycles. After this activation, the catalytic activity remained constant and well reproducible for the following runs. However, it is quite interesting that the samples need a reactivation process after they were put in the air for a relative long period. It is shown in Fig. 6(d) the activity results of the $Au/LaVO_4$ (5 nm, 3 wt%) composite after being placed in ambient air for 6 months. Once being reactivated, the composite showed an activity close to the origin value with only a minor decrease. Similar phenomena of Au/oxide catalyst which deactived after storage in ambient environments and could be regenerated upon high-temperature calcinations were also addressed by other publications, which is ascribed to the necessary process of removal of moisture and adsorbed impurities on the nanocomposites [34, 36].

3. Conclusions

In summary, a novel colloid-preparation route in nonpolar solvent for $Au/LaVO_4$ nanocomposite catalyst was developed successfully. Well-defined $LaVO_4$ NCs and monodispersed Au nanoparticles were pre-synthesized and dispersed in cyclohexane as building blocks of the nanocomposite. These $Au/LaVO_4$ nanocomposites have been catalytically evaluated for CO oxidation. Size effect of gold particles was investigated and the data confirm that the activity for CO oxidation is strongly dependent on the gold particle size. However, even if a full understanding of the systems is still lacking, the synthetic method described here and the analysis of the samples provide the basis for decoupling the influence of the support on the synthesis of the gold particles. This study based on non-oxide support gold composite might light new opportunities in the development of high-performance gold catalysts.

Acknowledgments

This work was supported by NSFC (50372030) and the state key project of fundamental research for nanomaterials and nanostructures (2003CB716901).

References

[1] Whitesides, G. M.; Grzybowski, B. Self-assembly at all scales. *Science* **2002**, *295*, 2418–2421.

[2] Daniel, M. C.; Astruc, D. Gold nanoparticles: Assembly, supramolecular chemistry, quantum-size-related properties, and applications toward biology, catalysis, and nanotechnology. *Chem. Rev.* **2004**, *104*, 293–346.

[3] Tauster, S. J.; Fung, S. C.; Garten, R. L. Strong metal-support interactions. Group 8 noble metals supported on titanium dioxide. *J. Am. Chem. Soc.* **1978**, *100*, 170.

[4] Chen, M. S.; Goodman, D. W. The structure of catalytically active gold on titania. *Science* **2004**, *306*,

252–255.

[5] Bell, A. T. The impact of nanoscience on heterogeneous catalysis. *Science* **2003**, *299*, 1688–1691.

[6] Haruta, M. Size- and support-dependency in the catalysis of gold. *Catal. Today* **1997**, *36*, 153–166.

[7] Hashmi, A. S. K.; Hutchings, G. J. Gold catalysis. *Angew. Chem.-Int. Edit.* **2006**, *45*, 7896–7936.

[8] Kung, H. H.; Kung, M. C.; Costello, C. K. Supported Au catalysts for low temperature CO oxidation. *J. Catal*. **2003**, *216*, 425–432.

[9] Lee, S. J.; Gavriilidis, A. Supported Au catalysts for low-temperature CO oxidation prepared by impregnation. *J. Catal*. **2002**, *206*, 305–313.

[10] Wolf, A.; Schuth, F. A systematic study of the synthesis conditions for the preparation of highly active gold catalysts. *Appl. Catal. A-Gen*. **2002**, *226*, 1–13.

[11] Zhou, K. B.; Wang, X.; Sun, X. M.; Peng, Q.; Li, Y. D. Enhanced catalytic activity of ceria nanorods from well-defined reactive crystal planes. *J. Catal*. **2005**, *229*, 206–212.

[12] Schlogl, R.; Abd Hamid, S. B. Nanocatalysis: Mature science revisited or something really new? *Angew. Chem.-Int. Edit*. **2004**, *43*, 1628–1637.

[13] Choudary, B. M.; Mulukutla, R. S.; Klabunde, K. J. Benzylation of aromatic compounds with different crystallites of MgO. *J. Am. Chem. Soc*. **2003**, *125*, 2020–2021.

[14] Chrzanowski, W.; Wieckowski, A. Surface structure effects in platinum/ruthenium methanol oxidation electrocatalysis. Langmuir **1998**, *14*, 1967–1970.

[15] Wang, X.; Zhuang, J.; Peng, Q.; Li, Y. D. A general strategy for nanocrystal synthesis. *Nature* **2005**, *437*, 121–124.

[16] Zhang, Y.; Jia, H. B.; Yu, D. P.; Luo, X. H.; Zhang, Z. S.; Chen, X. H.; Lee, C. Shape-controllable synthesis of indium oxide structures: Nanopyramids and nanorods. *J. Mater. Res*. **2003**, *18*, 2793–2798.

[17] Lee, H.; Habas, S. E.; Kweskin, S.; Butcher, D.; Somorjai, G. A.; Yang, P. D. Morphological control of catalytically active platinum nanocrystals. *Angew. Chem.-Int. Edit*. **2006**, *45*, 7824–7828.

[18] Fang, Z. M.; Hong, Q.; Zhou, Z. H.; Dai, S. J.; Weng, W. Z.; Wan, H. L. Oxidative dehydrogenation of propane over a series of low-temperature rare earth orthovanadate catalysts prepared by the nitrate method. *Catal. Lett*. **1999**, *61*, 39–44.

[19] Martinez-Huerta, M. V.; Coronado, J. M.; Fernandez-Garcia, M.; Iglesias-Juez, A.; Deo, G.; Fierro, J. L. G.; Banares, M. A. Nature of the vanadia-ceria interface in V^{5+}/CeO_2 catalysts and its relevance for the solid-state reaction toward $CeVO_4$ and catalytic properties. *J. Catal*. **2004**, *225*, 240–248.

[20] Liu, J. F.; Li, Y. D. Synthesis and self-assembly of luminescent Ln(3+)-doped $LaVO_4$ uniform nanocrystals. *Adv. Mater*. **2007**, *19*, 1118–1122.

[21] Liu, J. F.; Li, Y. D. General synthesis of colloidal rare earth orthovanadate nanocrystals. *J. Mater. Chem*. **2007**, *17*, 1797–1803.

[22] Ge, J. P.; Chen, W.; Liu, L. P.; Li, Y. D. Formation of disperse nanoparticles at the oil/water interface in normal microemulsions. *Chem.-Eur. J*. **2006**, *12*, 6552–6558.

[23] Tsubota, S.; Nakamura, T.; Tanaka, K.; Haruta, M. Effect of calcination temperature on the catalytic activity of Au colloids mechanically mixed with TiO_2 powder for CO oxidation. *Catal. Lett*. **1998**, *56*, 131–135.

[24] Grunwaldt, J. D.; Kiener, C.; Wogerbauer, C.; Baiker, A. Preparation of supported gold catalysts for low-temperature CO oxidation via "size-controlled" gold colloids. *J. Catal*. **1999**, *181*, 223–232.

[25] Comotti, M.; Li, W. C.; Spliethoff, B.; Schuth, F. Support effect in high activity gold catalysts for CO oxidation. *J. Am. Chem. Soc*. **2006**, *128*, 917–924.

[26] Li, J.; Zeng, H. C. Preparation of monodisperse Au/TiO_2 nanocatalysts via self-assembly. *Chem. Mater*. **2006**, *18*, 4270–4277.

[27] Hickey, N.; Larochette, P. A.; Gentilini, C.; Sordelli, L.; Olivi, L.; Polizzi, S.; Montini, T.; Fornasiero, P.; Pasquato, L.; Graziani, M. Monolayer protected gold nanoparticles on ceria for an efficient CO oxidation catalyst. *Chem. Mat*. **2007**, *19*, 650–651.

[28] Zheng, N. F.; Stucky, G. D. A general synthetic strategy for oxide-supported metal nanoparticle catalysts. *J. Am. Chem. Soc*. **2006**, *128*, 14278–14280.

[29] Schmid, G.; Corain, B. Nanoparticulated gold: Syntheses, structures, electronics, and reactivities. *Eur. J. Inorg. Chem*. **2003**, 3081–3098.

[30] Hussain, I.; Graham, S.; Wang, Z. X.; Tan, B.; Sherrington, D. C.; Rannard, S. P.; Cooper, A. I.; Brust, M. Size-controlled synthesis of near-monodisperse gold nanoparticles in the 1–4 nm range using polymeric stabilizers. *J. Am. Chem. Soc*. **2005**, *127*, 16398–16399.

[31] Shimizu, T.; Teranishi, T.; Hasegawa, S.; Miyake, M. Size evolution of alkanethiol-protected gold nanoparticles by heat treatment in the solid state. *J. Phys. Chem. B* **2003**, *107*, 2719–2724.

[32] Alvarez, M. M.; Khoury, J. T.; Schaaff, T. G.; Shafigullin, M. N.; Vezmar, I.; Whetten, R. L. Optical absorption spectra of nanocrystal gold molecules. *J. Phys. Chem. B* **1997**, *101*, 3706–3712.

[33] Bera, P.; Hegde, M. S. Characterization and catalytic properties of combustion synthesized Au/CeO_2 catalyst. *Catal. Lett.* **2002**, *79*, 75–81.

[34] Glaspell, G.; Hassan, H. M. A.; Elzatahry, A.; Fuoco, L.; Radwan, N. R. E.; El-Shall, M. S. Nanocatalysis on tailored shape supports: Au and Pd nanoparticles supported on MgO nanocubes and ZnO nanobelts. *J. Phys. Chem. B* **2006**, *110*, 21387–21393.

[35] Valden, M.; Lai, X.; Goodman, D. W. Onset of catalytic activity of gold clusters on titania with the appearance of nonmetallic properties. *Science* **1998**, *281*, 1647–1650.

[36] Zhu, H. G.; Ma, Z.; Clark, J. C.; Pan, Z. W.; Overbury, S. H.; Dai, S. Low-temperature CO oxidation on Au/fumed SiO_2-based catalysts prepared from $Au(en)_2Cl_3$ precursor. *Appl. Catal. A-Gen*. **2007**, *326*, 89–99.